Indian Journal of Biochemistry & Biophysics
Vol. 60, March 2023, pp. 209-223
DOI: 10.56042/ijbb.v60i3.63521

Some bis (3-(4-nitrophenyl)acrylamide derivatives: Synthesis, characterization, DFT, antioxidant, antimicrobial properties, molecular docking and molecular dynamics simulation studies

Şükriye Çakmak[1]* & Taner Erdoğan[2]

[1]Department of Medical Services and Techniques, Vocational School of Health Services, Sinop University, Sinop, Turkey

[2]Department of Chemistry and Chemical Processing Technologies, Kocaeli Vocational School, Kocaeli University, Kocaeli, Turkey

Received 23 May 2022; *revised 14 December 2022*

Alzheimer's disease, which is a progressive neurologic disorder, is the most common form of dementia. Although there are various treatment options for Alzheimer's disease, there is no definite treatment for this disease yet. In this study it was aimed to investigate the treatment potentials of three bis(3-(4-nitrophenyl)acrylamide) derivatives, two of which are known and one is new, for Alzheimer's disease. The study consists of three parts; in the first part of the study, synthesis and characterization studies of the investigated compounds were carried out. In the characterization of the compounds, IR, ^{1}H-NMR, ^{13}C-NMR, LC-MS and elemental analysis techniques were used. In the second part of the study, the compounds were investigated computationally with the assistance of various computational techniques including density functional theory (DFT) calculations, molecular docking and molecular dynamics simulations. In this part, binding free energy calculations were also performed on the investigated compounds. Results of computational studies showed that synthesized compounds interacted with AChE effectively and can be promising structures as AChE inhibitors. In the last part of the study, antioxidant and antimicrobial properties of the compounds were investigated. Antioxidant activities were determined by DPPH$^{\cdot}$ and ABTS$^{\cdot+}$ radical scavenging methods. According to the DPPH$^{\cdot}$ test, the most active compound was found to be 2, while the most active compound was found to be 3 according to the ABTS^{+} test, showing that these methods for antioxidant assay were not significantly correlated with each other. On the other hand, the results of the antimicrobial activity tests showed that compound 3 was the most active compound, which exhibited both antioxidant and antimicrobial activity.

Keywords: Acetylcholinesterase, AChE, Binding free energy, MM-PBSA, Spectroscopic elucidation

Alzheimer's disease (AD) is known to be a neurodegenerative brain disorder and causes many abnormalities such as problems with recognition, consideration and social behavior. Although there are some therapeutic options decelerating the progression of the disease or providing symptomatic relief, these options cannot provide a definite cure yet. Since acetylcholinesterase (AChE) plays an important role in AD, inhibition of this enzyme is one of the strategies used for the treatment of AD. In the literature there are some recent studies focus on the inhibition of AChE[1–6]. Computational tools such as molecular docking and molecular dynamics simulations are widely used in drug research and development studies, and many current studies in the literature use these methods[7-11]. Therefore, in the study it was aimed to investigate the AChE inhibition potentials of the synthesized compounds with the assistance of *in silico* methods.

The acrylamide moiety is an important component appears widely implicated in various biochemical processes and exhibits diverse pharmacological activities. In the literature numerous compounds containing an acrylamide moiety show widespread biological activities such as antiviral, antidiabetic[12], antibacterial[13], antitumor[14], antioxidant[15], antiproliferative[16]. This moiety is found in the structure of many approved drugs such as Entacapone, Panobinostat, Belinostat and Rifampicin[17].

In the study it was aimed to perform *in vitro* and *in silico* investigations on some bis(3-(4-nitrophenyl)acrylamide) derivatives for their possible antioxidant, antimicrobial and AChE inhibitory activity. Therefore, three bis(3-(4-nitrophenyl)acrylamide) derivatives, two of which are known (1 and 2) and one is new(3), have been synthesized, and characterized with the assistance of various spectroscopic techniques including IR, ^{1}H-NMR, ^{13}C-NMR, LC-MS and elemental analysis. Additionally, the synthesized

*Correspondence:
Phone: +90 368 27157 57-34 10
E-mail: scakmak@sinop.edu.tr
Suppl. Data available on respective page of NOPR

compounds were investigated *in silico* with the use of computational tools such as DFT calculations, molecular docking calculations, molecular dynamics simulations and binding free energy calculations to reveal their AChE inhibition potentials. Results showed that all synthesized compounds effectively bound to AChE and formed stable complexes, thus can be promising structures for AChE inhibition. Moreover, antioxidant activities of the compounds were determinedby DPPH$^{\cdot}$ and ABTS$^{\cdot+}$ radical scavenging methods. Additionally, they were also tested for their antimicrobial activity against three gram-positive bacteria (*B. cereus, S. aureus*, and *E. faecalis*) and three gram-negative bacteria (*E. coli, P. aeruginosa* and *K. pneumoniae*). In these tests, amoxicillin and tetracycline antibiotics were used as reference drugs.

Experimental Section

Instruments and reagents

All the chemicals and solvents used in the study were of reagent grade (Merck, Sigma-Aldrich) and used without further purification. IR spectra were recorded on Perkin Elmer FT-IR spectrometer. The ^{1}H-NMR and ^{13}C-NMR spectra were recorded on Bruker/Biospin 400 MHz spectrometer operating at 400 MHz using DMSO-d_6 as solvent and tetramethylsilane as internal standard. The splitting patterns were given as s (singlet), d (doublet), dd (doublet of doublets), t (triplet) and m (multiplet). In the determination of melting points, Stuart SMP 30 apparatus were used, and the uncorrected values of melting points were reported. Elemental analyses were performed using a Vario Elementar Microcube. Mass spectra were taken on a Shimadzu LCMS-8030 Plus LC- MS/MS spectrophotometer.

General procedure for the synthesis of bis(3-(4-nitrophenyl)acrylamide) derivatives (1-3)

The intermediate compound, trans-4-nitro cinnamoyl chloride, was prepared by a modified form of the procedure described in the literature[18]. The remaining acyl chloride was obtained as crude material, and was used in the subsequent reactions of bis(3-(4-nitrophenyl)acrylamide) derivatives without further purification or prior treatment. The synthetic pathway is given in (Scheme 1).

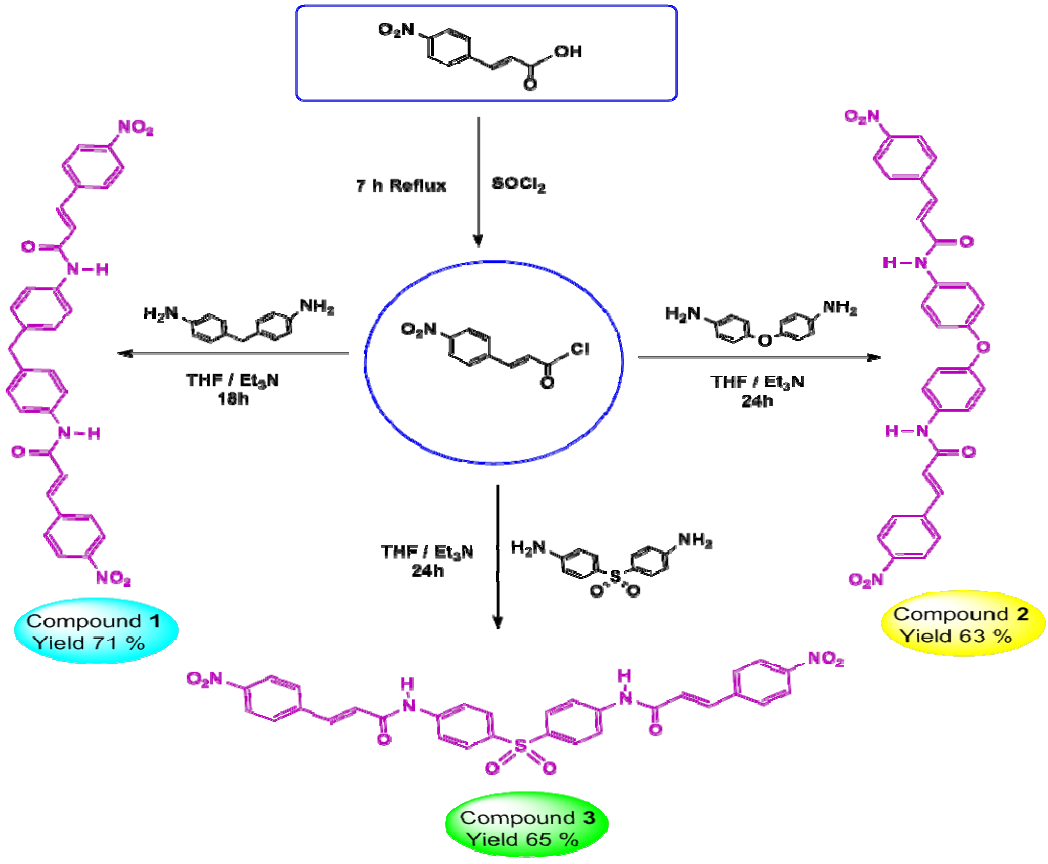

Scheme 1 — Synthetic route for bis(3-(4-nitrophenyl)acrylamide) derivatives (1-3)

The syntheses of bis(3-(4-nitrophenyl)acrylamide) derivatives (1-3) were carried out in a slightly basic medium by taking 2:1 ratio of acyl chloride and diamine derivative. The primary diamine derivative (0.004 mol) was dissolved in THF and triethylamine (Et_3N) (0.6 mL) then it was added dropwise to the reaction medium. The solution was made to be slightly basic. The solution of trans-4-nitro cinnamoyl chloride (0.01 mol) in THF was added dropwise to the reaction mixture with stirring. Then, the reaction mixture was stirred at 25°C for 18-24 h. The progress of the reaction was monitored by TLC. After completion of the reaction, the resulting salt precipitate was filtered off and the remaining filtrate was precipitated by adding water. The final product was filtered, washed with water, and recrystallized in a suitable solvent[19,20].

The synthesized compounds were characterized by analytical techniques such as IR, NMR, MS, *etc*. The characterization details are given as follows:

(2E,2'E)-*N,N'*-(methylenebis(4,1-phenylene))bis(3-(4-nitrophenyl) acrylamide,1

Bright yellow solid, Yield 71%, mp.246.91°C.FT-IR (ATR) (cm^{-1}): 3110 NH (Amide), 1681 C=O (Amide I), 1603 CONH (Amide II), 1520-1343 N=O (Asym.) N=O (Sym.), respectively, 1625 -HC=CH- (Olefinic bonds). ^{1}H NMR (400 MHz, DMSO-d_6)δ (ppm): 10.34 (s, 2H, -NH), 8.30-8.27 (d, 1H, Ar-H, aromatic protons of nitro substituted phenyl ring, H1), 7.99-7.97 (d, 1H, Ar-H, H2), 7.21-7.19 (d, Ar-H, H5), 6.67-6.73(d, Ar-H,H6), 7.72-7.68 and 7.65-7.61 (d, 2H, H3 and H4, olefinic protons), 3.87 (s, 2H, Ar-CH_2-Ar)^{13}C NMR (100 MHz, DMSO-d_6)δ (ppm): 167.59, 148.35, 141.78, 141.17, 129.73, 129.46, 129.15, 124.60, 124.36, 127.03 and 119.91.LC-MS/MS: 549.80$[M+H]^+$, calc. 548.56. Elemental analysis: Calculated for molecular formulae $C_{31}H_{24}N_4O_6$ Calculated: C, 67.88; H, 4.41; N, 10.21. Found: C, 67.40; H, 4.25; N, 10.12 (Suppl. Figs S1-S4).

(2E,2'E)-*N,N'*-(oxybis(4,1-phenylene))bis(3-(4-nitrophenyl) acrylamide), 2

Yellow solid, Yield 63%, mp.291.10°C.FT-IR (ATR) (cm^{-1}) : 3109 NH (Amide), 1689 C=O (Amide I), 1602 CONH (Amide II), 1520-1340 N=O (Asym.) N=O (Sym.), respectively, 1625 -HC=CH- (Olefinic bonds), 1111 Ar-O-Ar. ^{1}H NMR (400 MHz, DMSO-d_6)δ (ppm): 10.43 (s, 2H, -NH), 8.31-8.29 (d, 1H, Ar-H, H1) 8.25-8.23(d, 1H, Ar-H, H2), 7.72-7.68 (d, 1H, Ar-H, H5), 6.77-6.73 (d, 1H, Ar-H, H6), 8.25-8.23 and 7.72-7.68 (d, 2H, H3 and H4, olefinic protons). ^{13}C NMR (100 MHz, DMSO-d_6)δ (ppm): 167.35, 148.69, 139.32, 134.30, 131.24, 129.81, 129.68, 129.68, 125.11, 124.25, 121.43, 119.31.LC-MS/MS: 550.90$[M]^+$, calc. 550.53. Elemental analysis: Calculated for molecular formulae $C_{30}H_{22}N_4O_7$ Calculated: C, 65.45; H, 4.03; N, 10.18. Found: C, 65.28; H, 4.02; N, 10.07 (Suppl. Figs S5-S8).

(2E,2'E)-N,N'-(sulfonylbis(4,1-phenylene))bis(3-(4-nitrophenyl) acrylamide), 3

Cream solid, Yield 65%, mp.277, 35°C, FT-IR (ATR) (cm^{-1}): 3110 NH (Amide), 1689 C=O (Amide I), 1603 CONH (Amide II), 1339-1145 S-O (Asym.) S-O (Sym.), 1520-1341 N=O (Asym.) N=O (Sym.), respectively, 1623 -HC=CH- (Olefinic bonds). ^{1}H NMR (400 MHz, DMSO-d_6)δ (ppm): 10.81 (s, 2H, -NH), 8.27-8.24 (d, 1H, Ar-H, H1), 7.99-7.96 (d, 1H, Ar-H,H2), 7.72-7.68 (d, 1H, Ar-H, H5), 6.77-6.73 (d,1H, Ar-H, H6), 7.92-7.89 and 7.71-7.67 (d, H3 and H4, olefinic protons). ^{13}C NMR (100 MHz, DMSO-d_6)δ (ppm): 167.35, 148.72, 139.32, 134.32, 131.27, 129.80, 129.70, 129.33, 125.12, 124.26, 119.94. LC-MS/MS: 598.75$[M]^+$, calc. 598.59. Elemental analysis: Calculated for molecular formulae $C_{30}H_{22}N_4O_8S$ Calculated: C, 60.20; H, 3.70; N, 9.36; S, 5.36. Found: C, 60.08; H, 3.65; N, 9.29; S, 5.29 (Suppl. Fig. S9).

DFT calculations

In this part of the study, geometry optimizations, frequency analyses, FMO (frontier molecular orbital)and MEP (molecular electrostatic potential) map calculations were performed on the synthesized compounds. In the calculations, Gaussian 09 Rev. D01[21], GaussView 5[22], VeraChem Vconf[23] software packages were used. Discovery Studio Visualizer[24] was used in the visualization of the results. Calculations were performed with the use of APF-D (Austin-Frisch-Petersson functional with dispersion) method and 6-311+G(2d,p) basis set. In the calculations, Polarizable Continuum Model using the integral equation formalism variant (IEFPCM) was used and water was selected as solvent.

***In vitro* antioxidant assay**

DPPH (1,1-diphenyl-2-picryl-hydrazyl) free radical scavenging activity

In vitro antioxidant assay was performed through slight modifications in DPPH free radical scavenging methods. The free radical scavenging activities of DMSO solutions of the synthesized compounds were

determined using DPPH$^{\cdot}$ (1.1-diphenyl-2-picrylhydrazil)[25]. For this, 150 µL of sample solutions at different concentrations and 50 µL of 0.1 mM DPPH$^{\cdot}$ were mixed homogeneously in a 96-well plate and left in the dark for 30 min at room temperature, 25°C. The absorbances of each mixture were measured at 517 nm using BIOTEK (Epoch2) microplate reader and the IC_{50} (µg/mL) values were determined. Butylated hydroxyanisole (BHA), *tert*-butylhydroquinone (TBHQ) and *α*-tocopherol were used as reference.

ABTS (2,2' -azino-bis(3-ethylbenzothiazoline-6-sulphonic acid) activity

$ABTS^{\cdot+}$ radical scavenging activities of the samples were calculated using the ABTS-K_2SO_8 method[26,27]. 7 mM ABTS and 2.45 mM K_2SO_8 (2:1) were mixed and incubated for 12-16 h at rt in the dark. The mixture was diluted with ethanol and the absorbance was found to be 0.700±0.020. In the 96-well plate, 20 µL of sample solution at different concentrations were mixed homogeneously with 180 µL of $ABTS^{\cdot+}$ solution. After 6 min, the absorbance of each mixture was measured at 734 nm using BIOTEK (Epoch2) microplate reader and the results were determined by calculating the IC_{50} (µg/mL) values. BHA, TBHQ and α-tocopherol were used as standards for the activity assay and the results were compared.

***In vitro*anti-microbial activity assay**

Determination of minimum inhibitory concentrations (MIC)

The antimicrobial activities of the target compounds were determined against *Escherichia coli* ATCC 25922^T, *Pseudomonas aeruginosa* ATCC 15442^T, *Klebsiella pneumoniae* ATCC 10031^T as gram negative bacteria and *Enterococcus faecalis* ATCC 29212^T, *Bacillus cereus* CCM 99^T, *Staphylococcus aureus* ATCC 25213^T as gram positive bacteria. Amoxicillin and tetracycline antibiotics were used as reference drugs.

The antibacterial activities of the synthesized compounds were determined by microbroth dilution method[28]. For cationic MHB (Mueller Hinton II Broth), 400 µL $MgCl_2$ (2 mg/mL) and 1 mL $CaCl_2$ (2 mg/mL) were added to 100 mL MHB. 100 µL of cationic MHB was added to each well in a sterile 96-well plate. 100 µL of sample (1024 µg/mL) or reference antibiotics amoxicillin (2048 µg/mL) and tetracycline (1024 µg/mL) were added to the first well, mixed and serial dilution was made up to well 12. Finale, 100 µL of solution from well 12 was discarded. 1 mL of the McFarland 0.5 bacterial solution was taken and mixed with 9 mL of cationic MHB and 5 µL of this solution was added to all wells. It was kept in a refrigerator at +4°C for 2 h and then it was left to incubate at 37°Cor 16-18 h. Minimum inhibitory concentrations (MIC) were given in µg/mL.

Molecular docking and molecular dynamics simulation studies

AutoDock Tools[29], AutoDock Vina[30] and Discovery Studio Visualizer[24] software packages were used in molecular docking calculations. The structure of acetylcholinesterase (AChE) was obtained from RCSB Protein Data Bank (PDB ID: 1eve)[31,32] and 3D structures of the investigated compounds were obtained from DFT calculations. Prior to molecular docking calculations, receptor was prepared by removing water molecules and bound ligands, then adding hydrogens and Gasteiger charges. Calculations were performed in a 20×20×20 $Å^3$ grid box covering active site of the enzyme and grid spacing was set to 1 Å. In molecular docking calculations Lamarckian genetic algorithm was used to obtain top-scoring docking poses for each compound.

After performing molecular docking calculations, a 100ns molecular dynamics simulation was performed for each top-scoring ligand-receptor complex to simulate the behavior of each complex and subsequently to determine the binding free energies. Molecular dynamics simulations were performed using GROMACS[33], AMBER force field[34] and TIP3P water model. Acpype Server[35] was used to obtain ligand topologies. Before performing molecular dynamics simulations, system was neutralized, and energy minimization was carried out by employing steepest descent minimization algorithm. 100 ns molecular dynamics simulations performed at 1 bar and 300 K reference pressure and temperature followed the 200 ps NVT and NPT ensemble equilibrations. After performing molecular dynamics simulations, MM-PBSA (Molecular Mechanics Poisson-Boltzmann Surface Area) calculations[36,37] were performed to determine the average binding free energies. In MM-PBSA calculations, the last 20 ns of each molecular dynamics simulation was used.

Statistical analysis

The triplicate analyzes results obtained from *in vitro* biological activity determination studies were expressed as ± standard deviation values for each parameter. IBM Statistical Package for Social Studies

(SPSS) 20.0 software package program was used to determine the differences between the groups using ANOVA.

Results and Discussion

IR spectra analysis

In the characterization of the synthesized bis (3-(4-nitrophenyl)acrylamide derivatives, IR spectral data were used. When the IR spectra are examined for all compounds (1-3), it was seen that the N-H stretching vibration was appeared in the range of 3109-3110 cm^{-1}, the amide I (C=O stretching) bands between 1689 cm^{-1} and 1681 cm^{-1}, and the bands 1603-1602 cm^{-1} region, due to the interaction of the N-H bending and C-N stretching referred to as the amide II bands. The absorption bands were observed in the range of 1343-1340 cm^{-1} and 1520 cm^{-1}, which are attributed to the symmetric and asymmetric stretching vibrations of N=O, respectively. In the spectra of 1-3, the bands at 1625 and 1623 cm^{-1} correspond to the stretching vibration of olefinic double bonds (–CH=CH-CO). Also, for compound 2, Ar-O-Ar symmetric stretching band was observed at 1111 cm^{-1}. The presence of these characteristic peaks in the IR spectra confirmed that the synthesized compounds were obtained successfully, as expected (Suppl. Figs S1 and S5).

In the spectrum of compound 3, the N-H stretching vibration was appeared at 3110 cm^{-1}, while the C=O stretching vibration (amide I) was appeared at 1689 cm^{-1}. The absorption bands observed at 1603 cm^{-1} indicated the interaction of the N-H bending and C-N stretching vibrations (amide II). In addition, this compound gave two bands around 1341 cm^{-1} and 1520 cm^{-1} due to the asymmetric and symmetric N=O stretching. Due to the symmetric and asymmetric vibrations of S-O bond of the sulfone group, two prominent bands were observed for compound 3, one of them appeared at 1145 cm^{-1} and the other at 1339 cm^{-1}. The olefinic double bond (–CH=CH-CO) stretching vibration peak was observed at 1623 cm^{-1}, as shown in (Fig. 1). IR spectral data of all compounds are also given in the supplementary material (Suppl. Figs S1 & S5). These spectral data are in good agreement with the values published previously for similar compounds[38–41].

^{1}H NMR spectra analysis

^{1}H NMR spectra of the synthesized compounds were taken in DMSO-d_6 and chemical shifts and multiplicities were correlated with the proposed structures. For compounds 1-3, the characteristic NH peaks appeared in the range of 10.81-10.34 ppm. The olefinic protons showed two doublet signals, one in the range of 8.25-7.89 ppm and the other at 7.72-7.61 ppm, respectively. The new peak appearing as singlet at 3.87 ppm was assigned to the methylene (Ar-CH_2-Ar) protons of compound 1. The aromatic ring protons resonated within the range of 8.25-6.72 ppm (Suppl. Figs S2 & S6).

In the ^{1}H NMR spectrum of compound 3 (Fig. 2), the NH peak was appeared as a singlet at 10.81 ppm. The H1 proton coupled with the H2 proton showed doublet at 8.27-8.24 and gave another doublet at 7.99-7.96 ppm, respectively. The other aromatic ring protons, H5 coupled with H6and gavetwo doublets at 7.72-7.68 ppm and 6.77-6.73 ppm, respectively. Two doublets were observed at 7.92-7.89 and 7.71-7.67

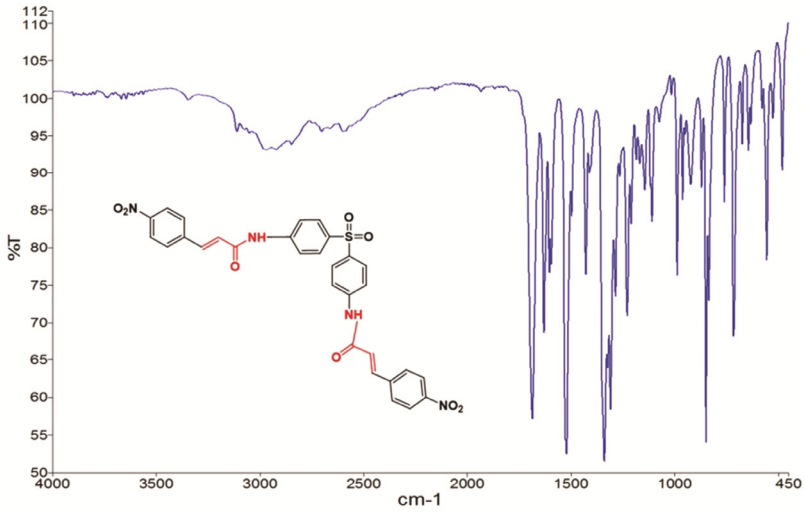

Fig. 1 — IR spectrum of compound3

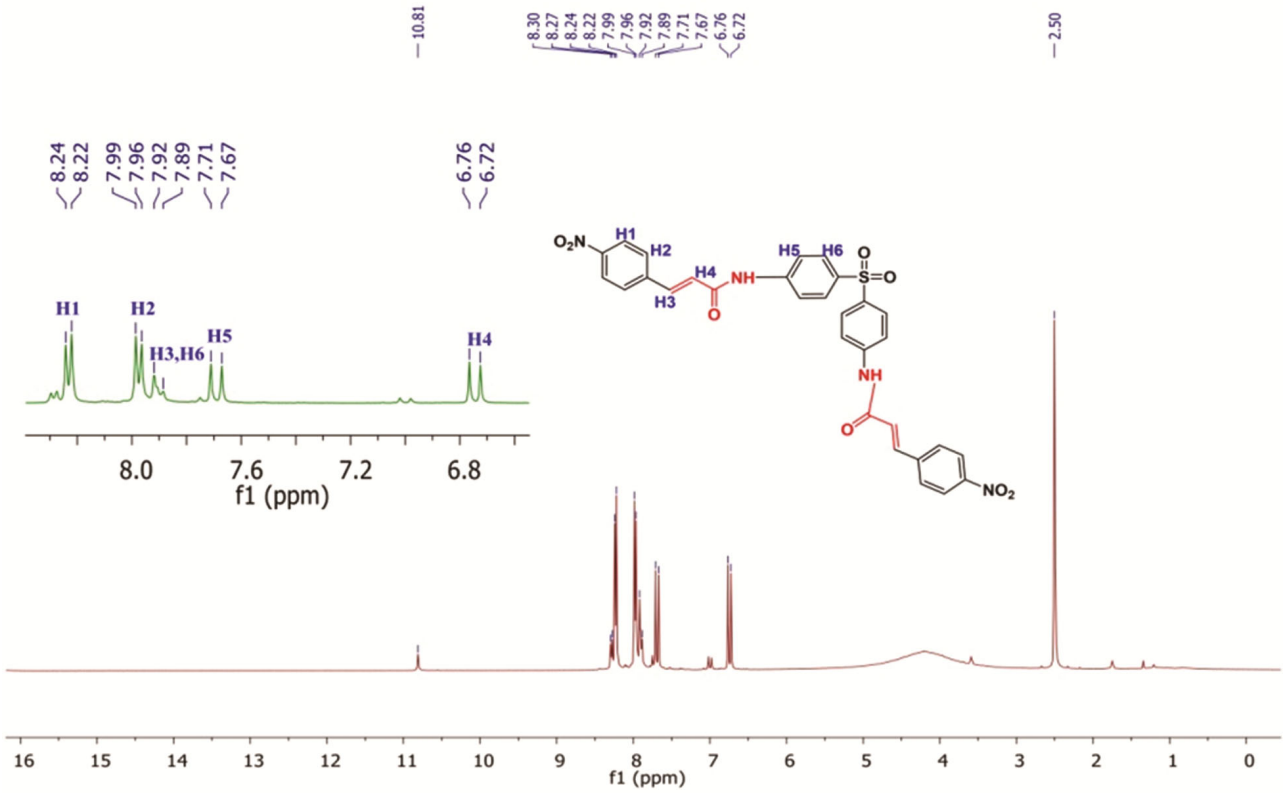

Fig. 2 — ^{1}H NMR spectrum of compound 3

ppm for olefinic protons H3 and H4, respectively. These results are consistent with the literature results for similar compounds[38–41].

^{13}C NMR spectra analysis

The ^{13}C NMR spectrum of the compound 3 showed 11 distinct resonances in accordance with the proposed structure as shown in (Fig. 3). The carbon signal belongs to theamide carbonyl carbon -C=O (C7) was appeared at 167.35 ppm. The signals belong to aromatic carbon (C1-C4) appeared at148.72, 125.12, 129.70, and 134.32 ppm while the signals for the other aromatic ring carbons (C8-C11) were appeared at 131.27, 119.94, 129.33 and 129.80 ppm, respectively. The two olefinic carbons (C5 and C6), adjacent to the amide carbonyl carbon resonated at 139.32 and 124.26 ppm, respectively.

In the spectra of compounds (1 and 2), the amide carbonyl carbon(C7) peaks were observed at 167.59 and 167.35 ppm, respectively. The olefinic carbons, C5 and C6, of compounds 1 and 2 resonated in the range of 141.78 -119.91 and 134.30-121.43 ppm, respectively. The aromatic carbons (C1-C4) resonated at 148.69-124.36 ppm, while the signals of other aromatic carbons (C8-C11) in the structure were observed in the range of139.32-119.31 ppm. Also, the CH_2 (C12) peak, which was expected to appear about 40.3 ppm, could not be observed for compound 1, probably due to the overlap with the DMSO peak. All synthesized compounds showed their characteristic signals and confirmed their proposed chemical structures (Figs S3 & S7). Spectral data of the compounds are in full agreement with the values reported previously for similar compounds[38–41].

DFT calculations

Geometry optimized structures of the investigated compounds obtained with the use of DFT/APF-D method and 6-311+G(2d,p) basis set are given in (Fig. 4).

A conformational search and a frequency analysis for each optimized geometry were performed to confirm that global minima were obtained for each optimized geometry. Performing conformational search and the absence of the imaginary frequency verified that each optimized geometry corresponds to a global minimum. Geometric parameters and vibrational spectra of the investigated compounds obtained from calculations performed with the use of APF-D method and 6-311+G(2d,p) basis set are given in Supplementary Information (Tables S1-S3 & Figs S10-S12).

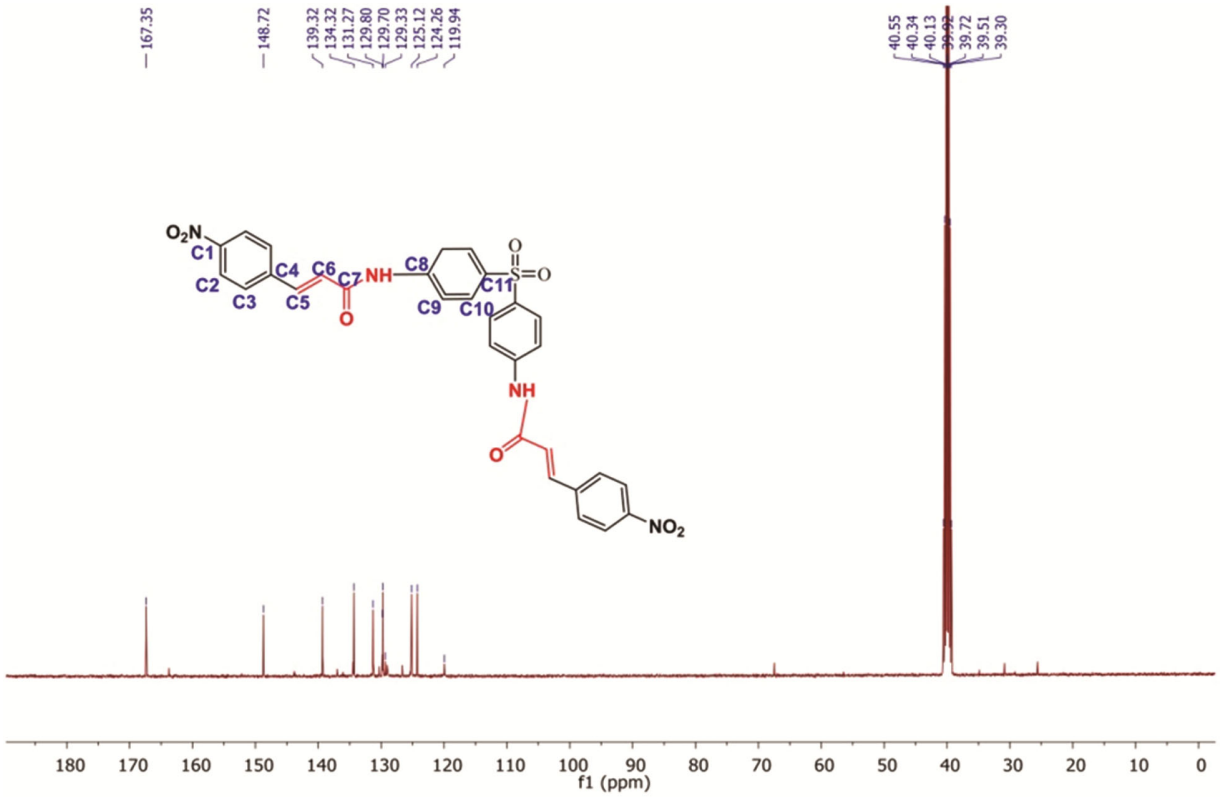

Fig. 3 — ^{13}C NMR spectrum of compound 3

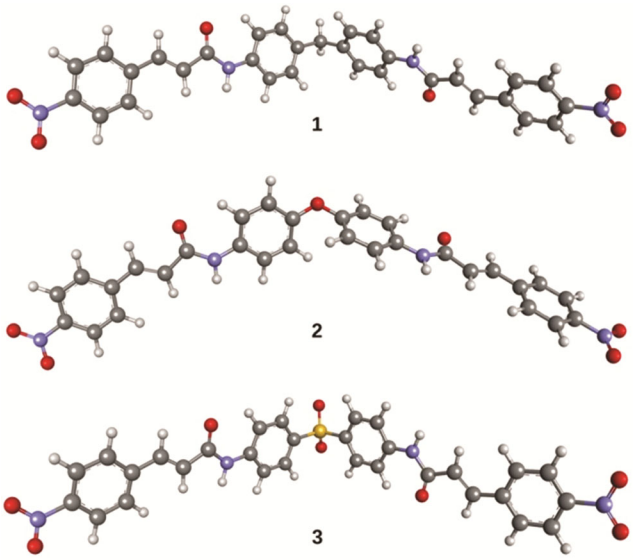

Fig. 4 — Geometry optimized structures of the synthesized compounds

HOMO (highest occupied molecular orbital) and LUMO (lowest unoccupied molecular orbital) of the investigated compounds, and HOMO-LUMO gaps are given in (Fig 5). HOMO-LUMO gaps of the synthesized compounds 1-3 were found to be 3.1257, 2.8918 and 3.4969 eV, respectively. Since the larger HOMO-LUMO gaps correspond to more stable structures, it was concluded that compound 3 is the most stable structure while compound 2 is the least stable one.

In Figure 6, MEP maps of the synthesized compounds obtained from DFT calculations are given. MEP maps of the compounds were obtained with the use of APF-D method, 6-311+G(2d,p) basis set and IEFPCM (The Polarizable Continuum Model PCM using the integral equation formalism variant) solvation model. MEP maps give information about the electron-rich and electron-deficient parts of a given molecule. Results showed that negative charge dominantly located on the oxygen atoms while positive charge located on the hydrogen atoms of N-H groups. Molecular docking and molecular dynamics simulation results also showed that these negative and positive regions of the compounds took part in the interactions formed between ligands and AChE.

In vitro antioxidant evaluation

DPPH and ABTS free radical scavenging ability of bis (3-(4-nitrophenyl)acrylamide derivatives

DPPH and ABTS are regarded as free radical generators and widely used to quantify antioxidative capacities of biological samples and food stuff. In this

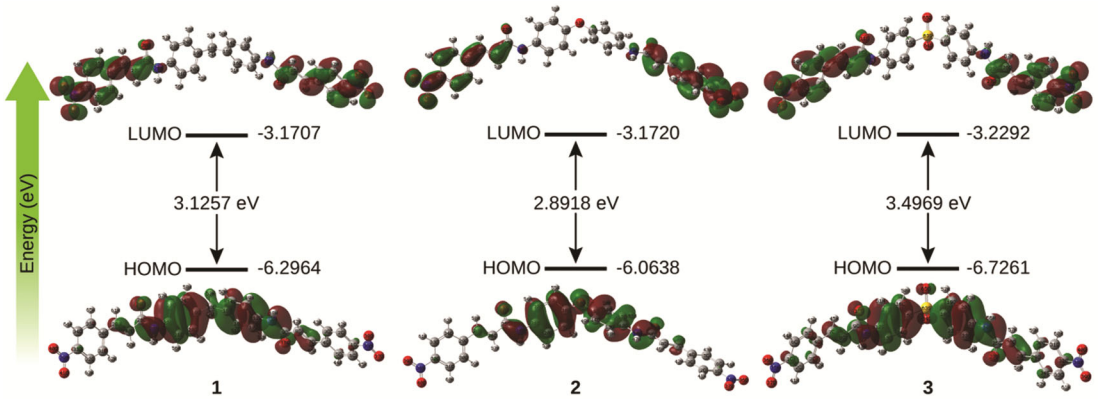

Fig.5 — FMOs of the synthesized compounds

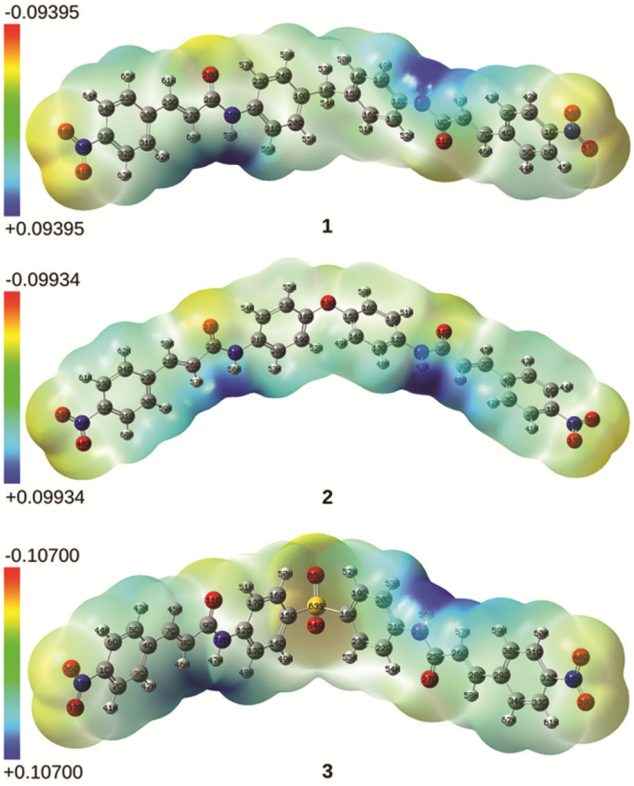

Fig.6 — MEP maps of the synthesized compounds

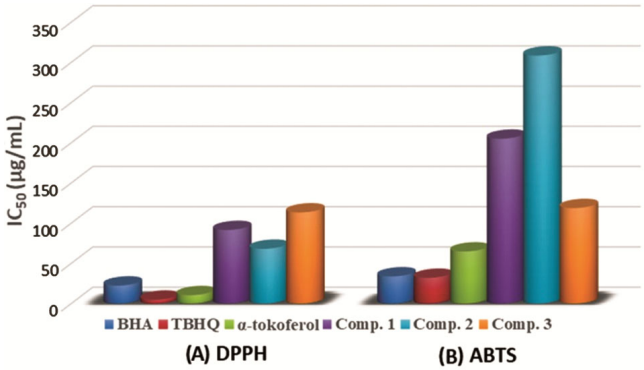

Fig. 7 — (A) DPPH; and (B) ABTS free radical scavenging capacities (IC_{50}) of bis (3-(4-nitrophenyl) acrylamide derivatives (1-3) and reference antioxidants

Table 1 — The antioxidant activities of bis (3-(4-nitrophenyl)acrylamide derivatives

Compounds	Antioxidant Activity, IC_{50} (µg/mL)	
	$DPPH^{\cdot}$	$ABTS^{\cdot+}$
1	91.64±0.46^{d}	308.66±1.60^{d}
2	68.26±1.04^{c}	205.18±4.26^{e}
3	113.39±0.82^{e}	118.88±1.16^{c}
BHA	22.54±0.24^{b}	33.91±2.09^{a}
TBHQ	4.82±0.24^{a}	32.09±2.02^{a}
α-tocopherol	10.56±1.66^{a}	64.86±3.28^{b}

NU: No use, The letters a, b, c, d and e are statistically significant indicators

study, the antioxidant properties of the investigated compounds (1-3) were evaluated through, $ABTS^{\cdot+}$ and $DPPH^{\cdot}$ scavenging activity. The results of antioxidant activity screening are given in (Table 1 and Fig. 7).

All the tested compounds were found to possess comparatively lower scavenging potential against DPPH radical in comparison to the standards, BHA, TBQH and α-tocopherol. These results can be explained by deactivation of the aromatic rings due to the electron- withdrawing effect of the nitro group[41,42]. As shown in (Fig. 7A), compound 2, which bears an oxydibenzene moiety, has the highest $DPPH^{\cdot}$ scavenging effect (IC_{50} 68.26±1.04 µg/mL). However, compound 3 showed the lowest activity (IC_{50} 113.39 ± 0.82 µg/mL) due to the presence of a sulfone group on the diamide skeleton. The order of the antioxidant activities of the investigated compounds and the reference molecules is as follows: TBHQ>α-tocopherol>BHA>2>1>3.

As shown in Figure 7B, the order of the $ABTS^{\cdot+}$ scavenging activities of the investigated compounds is

Table 2 — The MIC values of bis (3-(4-nitrophenyl)acrylamide derivatives (1-3) and standards

Compounds	Minimum Inhibiton Concentration (µg/mL)					
	Gram-negative bacteria			Gram-positive bacteria		
	E. coli (ATCC 25922)	*P. aeruginosa* (ATCC 15442)	*K. pneumoniae* (ATCC 10031)	*E. faecalis* (ATCC 29212)	*B. cereus* (CCM 99)	*S. aureus* (ATCC 25213)
1	512	1024	512	512	512	512
2	128	256	256	128	128	128
3	64	128	64	64	64	64
Amoxicillin	>1024	>1024	>1024	>1024	>1024	>1024
Tetracycline	64	64	64	64	4	64

as follows: 3>2>1. Considering the molecules, compound 3 (IC_{50} 118.88±1.16 µg/mL) is the most active compound, whereas compound 1 (IC_{50} 308.66±1.60 µg/mL) the least active compound. As a result, it was revealed that all tested compounds showed low antioxidant activity compared to the standards, BHA, TBQH and α-tocopherol. No correlation was found by comparing the $DPPH^{\cdot}$ with $ABTS^{+}$ assays, therefore, no general statement can be drawn for the assays. According to the results of both tests, the presence of the substituents in the structure of the compounds have a negative effect on the $DPPH^{\cdot}$ scavenging activity. However, a similar trend was not observed for $ABTS^{+}$ scavenging assay.

***In vitro* antimicrobial activity evaluation**

All the synthesized compounds were screened for their antibacterial activity against three Gram-negative bacteria *E. coli*, *P. aeruginosa* and *K. pneumoniae*, three Gram-positive bacteria *E. faecalis*, *B. cereus* and *S. aureus* by determination of the MIC values using microbroth dilution method. Reference drugs Amoxicillin and Tetracycline were also tested under similar conditions for comparison. The minimum inhibitory concentration (MIC) of the synthesized compounds and standards are reported in (Table 2). Among the compounds tested, compound 3 was found to be the most potent molecule with the MIC value of 64 µg/mL for all micro-organisms except *P. aeruginosa.* The relatively higher antimicrobial activity of compound 3 can be explained by the presence of sulfone group in the structure of this compound. Compound 2, which is the second most active one, was found to be approximately four times more active than compound 1 against some certain bacterial species. The antibacterial activity evaluation is largely dependent on the type of the various substituents in the structure and the amide moiety[42,43].

Molecular docking and molecular dynamics simulation studies

In molecular docking calculations, initial top-scoring binding positions of the synthesized compounds and reference drug donepezil were obtained. After performing molecular docking calculations, each top-scoring ligand-receptor complexes were subjected to 100 ns molecular dynamics simulation aiming to investigate the stability of ligand-receptor complexes and the interactions between ligands and receptor. RMSDs (root mean square deviations) of ligands after least square fit to protein were monitored during the molecular dynamics simulations and are given in (Fig 8). Results for AChE-1 complex showed that ligand reached its equilibrium position in the binding pocket around 10^{th} ns of the simulation and no significant change in the relative position of the ligand was observed in the remaining time of the simulation. Results for AChE-2 complex showed that ligand reached its equilibrium position immediately and kept its position throughout the entire simulation. Results for AChE-3 complex showed that ligand reached its equilibrium position around 10^{th} ns. Although there was a slight change in the position of the ligand around 80^{th} ns, it was observed that ligand remained bound in the binding pocket of AChE during the entire simulation. Results also showed that in AChE-donepezil complex, donepezil could not equilibrate before 45^{th} ns of the simulation but in the remaining time of the simulation no considerable change was observed (Fig. 8).

RMSD and RG (radius of gyration) of protein are known to be good indicators of stability, thus, RMSD of protein backbone and RG of protein were also monitored during the molecular dynamics simulation for all ligand-receptor complexes and are given in (Figs 9 & 10). Since there were no significant change in RMSD of backbone and RG of protein during the simulation, it was concluded that the enzyme

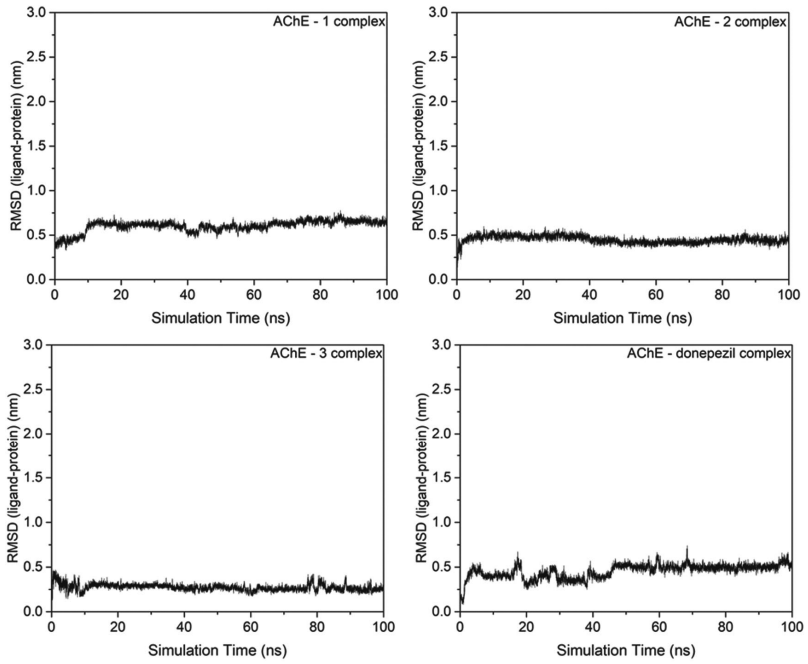

Fig.8 — RMSDs of the ligands after least square fit to protein for AChE-ligand complexes

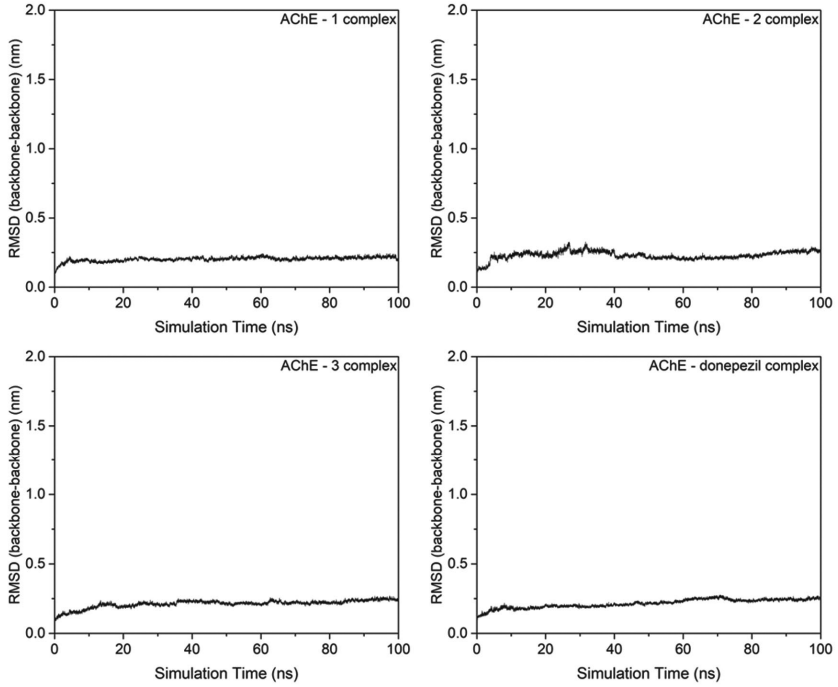

Fig.9 — RMSDs of the protein after least square fit to protein for all AChE-ligand complexes

remained stable in all ligand-receptor complexes. Average RGs of proteins and standard deviations were found to be 2.3456 nm (0.0098), 2.3528 nm (0.0087), 2.3453 nm (0.0075) and 2.3440 nm (0.0074) for AChE-1, AChE-2, AChE-3 and AChE-donepezil complexes, respectively.

In molecular dynamics simulation studies, number of hydrogen bonds formed between ligands and AChE were also monitored during the simulation and are given in (Fig 11). Results showed that the highest number of hydrogen bonds was observed for AChE-2 complex while the lowest one was observed for

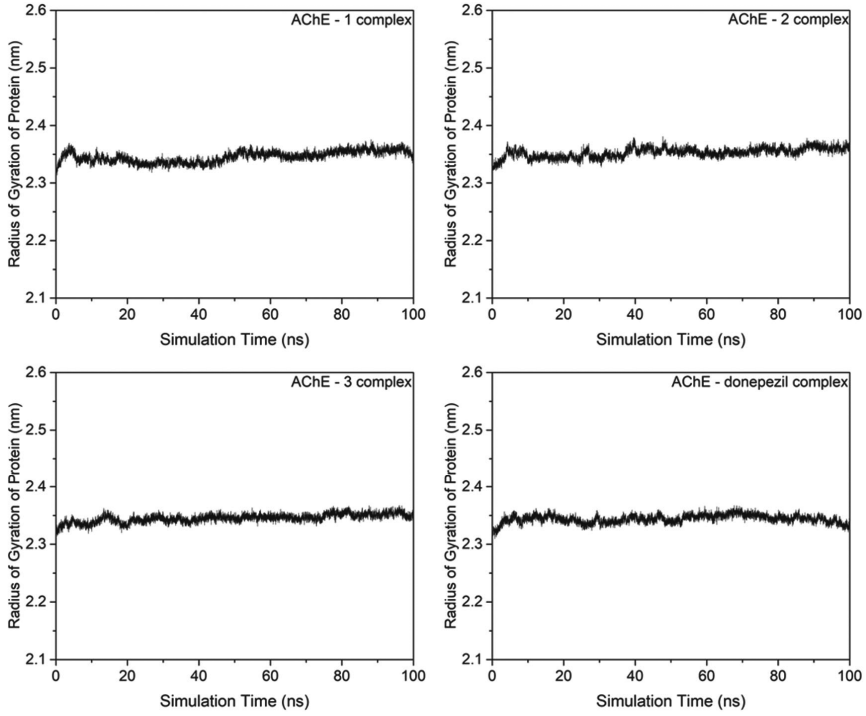

Fig. 10 — RG of proteins during the molecular dynamics simulation

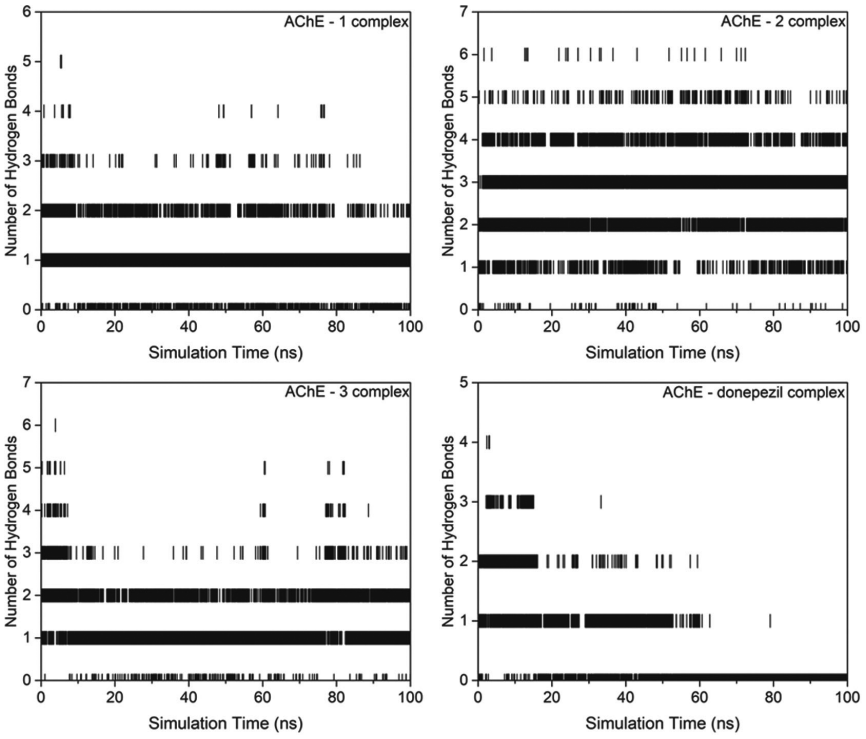

Fig.11 — Number of hydrogen bonds formed during the molecular dynamics simulation binding positions of the synthesized compounds and interactions between ligands and AChE belong to the 100th ns of molecular dynamics simulations are given in Figs 12 and 13. Results showed that PHE75, TRP84, SER124, PHE284, ASP285, ILE287, ARG289, TYR334, VAL71, PRO76, GLY77, PHE78, PRO86, GLY117, GLY118, TYR121, GLY123, LEU282, SER286 and especially TYR70, TRP279, and PHE288 amino acids took part in the interactions between ligands and AChE

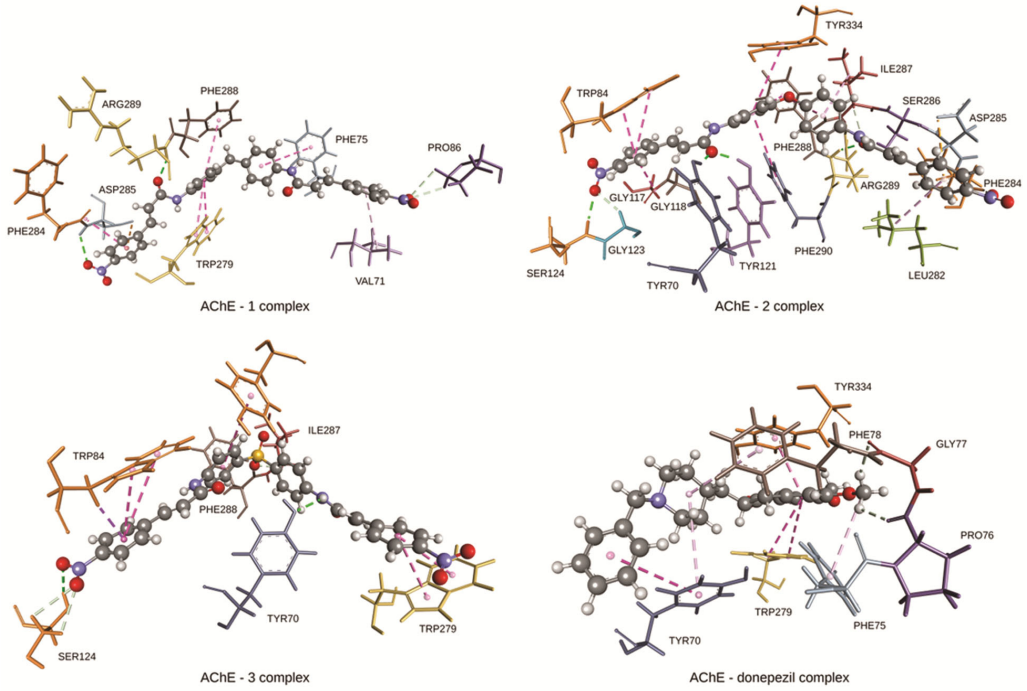

Fig.12 — Interactions between ligands and AChE

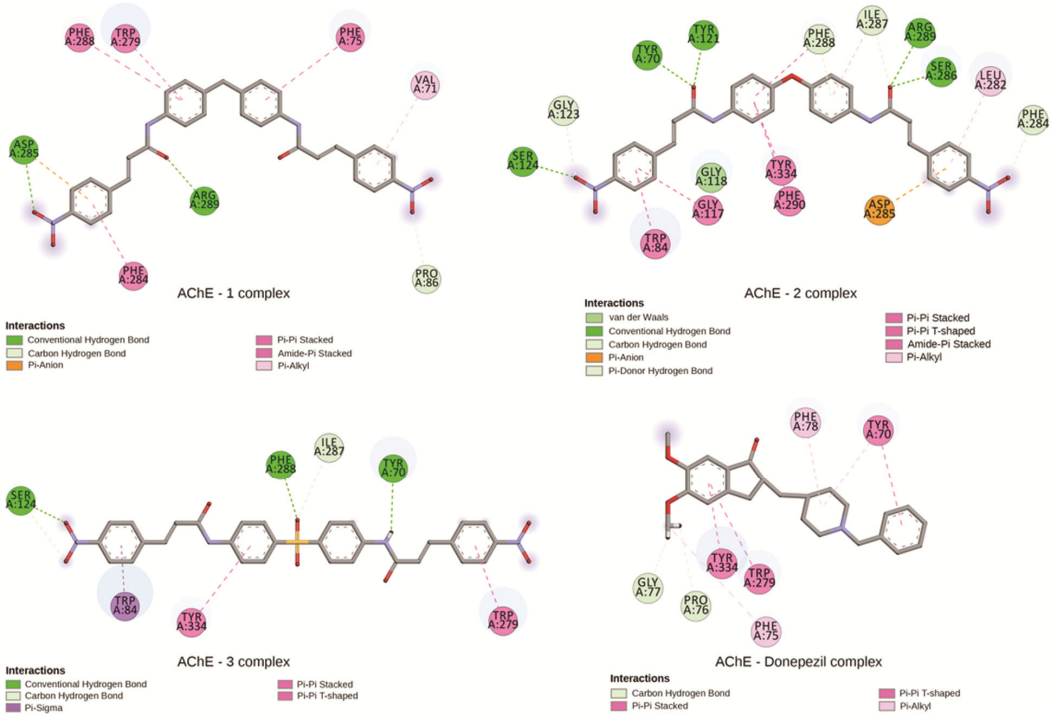

Fig. 13 — 2D Representation of the interactions between ligands and AChE

AChE-1 complex. On the other hand, it was observed that the number of hydrogen bonds formed between compounds 1-3 and AChE was found to be higher than that of formed between donepezil and AChE. Average number of hydrogen bonds were found to be 1.108, 2.764, 1.323 and 0.555 for AChE-1, AChE-2, AChE-3 and AChE-donepezil complexes, respectively (Figs 12 & 13).

In the study, binding free energies of the investigated compounds have also been calculated

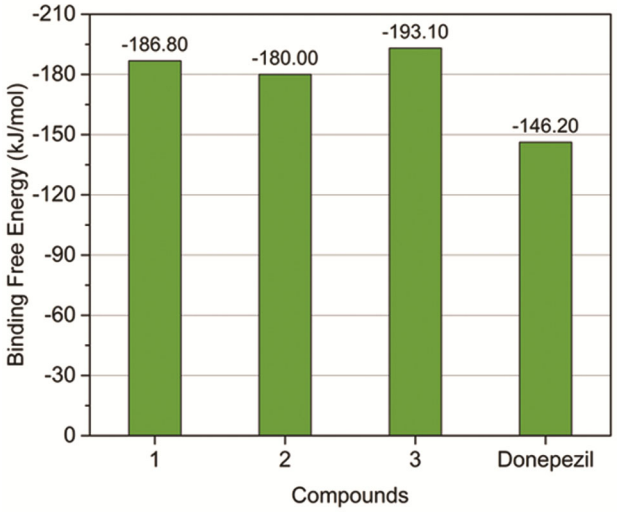

Fig. 14 — Binding free energies of the investigated compounds

with the use of MM-PBSA method. Results showed that all synthesized compounds have higher binding affinity than reference drug donepezil, and compound 3 has the highest binding affinity to AChE (Fig. 14). When compared with similar studies in the literature[44,45] and the reference drug Donepezil, these values are seen to be quite good, and the compounds can have high AChE inhibition potential.

Conclusion

In this study, three bis(3-(4-nitrophenyl)acrylamide) derivatives, two of which are known and one is new, were synthesized and characterized with the use of various spectroscopic techniques and then evaluated for their antioxidant activity with the use of two methods. The antioxidant capacities were determined by DPPH (IC_{50} values range from 68.26 to 113.39 µg/mL) and ABTS (IC_{50} values range from 118.88 to 308.66 µg/mL) assays. The $DPPH^{\cdot}$ scavenging effects of the compounds, especially compound 2 (IC_{50} 68.26±1.04 µg/mL), which is carrying an oxydibenzene moiety in the structure, has the highest activity but almost all compounds showed less antioxidant activity than the corresponding standards. This effect is related to the presence of the electron-withdrawing nitro group in the structures of all compounds. The order of $ABTS^{+}$ scavenging activities was found to be as follows: 3>2>1. On the other hand, obtaining the lowest $DPPH^{\cdot}$ scavenging activity for compound 3 revealed that there was no clear correlation between $ABTS^{\cdot+}$ and $DPPH^{\cdot}$ tests. Also, all the compounds were tested for antibacterial activity using three gram-positive and three gram-negative bacteria. Among the compounds tested, compound 3 exhibited exceptionally good antimicrobial activities compared to other derivatives against all micro-organisms except *P. aeruginosa* bacterial specie with MIC values of 64 µg/mL and even showed activity equal to Tetracycline antibiotic. The increase in antimicrobial activity can be explained by the presence of the sulfone group in this compound. The results revealed that compound 3 has both antioxidant and antimicrobial activity. Compound 2, which is the second most active one, was found to be approximately four times more active than compound 1 against some certain bacterial species. The degree of antibacterial activity is largely dependent on the type of the substituents the structures bear and the presence of amide moiety.

Additionally, these synthesized compounds were investigated for their AChE inhibition potentials with the use of computational tools including DFT calculations, molecular docking calculation, molecular dynamics simulation studies and binding free energy calculations. Results showed that the binding affinities of the synthesized compounds are higher than that of reference drug donepezil. Since the synthesized compounds have considerably high binding affinity to AChE and form stable complexes with AChE, it was concluded that the synthesized compounds are promising structures as AChE inhibitors, and it is worth for further investigations.

Acknowledgement

The computational studies reported in this paper were partially performed at TUBITAK ULAKBIM, High Performance and Grid Computing Center (TRUBA resources) and Kocaeli University. Moreover, authors thank Prof. Dr. TevfikÖzen (Chemistry Department, OndokuzMayis University) for his help in performing the antioxidant and antimicrobial activity assays.

Conflict of interest

All authors declare no conflict of interest.

References

1 Bhagat K, Singh JV, Sharma A, Kaur A, Kumar N, Gulati HK, Singh A, Singh H & Bedi PMS, Novel series of triazole containing coumarin and isatin based hybrid molecules as acetylcholinesterase inhibitors. *J Mol Struct*, 1245 (2021) 131085.

2 Bilginer S, Gul HI, Hanci H & Gulcin I, Antibacterial and acetylcholinesterase inhibitory potentials of triazenes containg sulfonamide moiety. *Pharm Chem J*, 55 (2021) 284.

3 Danish M, Raza MA, Rani H, Akhtar A, Arshad MN & Asiri AM, Enzyme inhibition and antioxidant potential of

new synthesized sulfonamides; synthesis, single crystal and molecular docking. *J Mol Struct*, 1241 (2021) 130608.

4 Zafar R, Zubair M, Ali S, Shahid K, Waseem W, Naureen H, Haider A, Jan MS, Ullah F, Sirajuddin M & Sadiq A, Zinc metal carboxylates as potential anti-Alzheimer's candidate: *in vitro* anticholinesterase, antioxidant and molecular docking studies, *J Biomol Struct Dyn,*39 (2020) 1044.

5 Macha B, Kulkarni R, Bagul C, Garige AK, Akkinepally R & Garlapati A, Molecular hybridization based design and synthesis of new benzo[5,6]chromeno[2,3-b]-quinolin-13(14H)-one analogs as cholinesterase inhibitors. *Med Chem Res*, 30 (2021) 685.

6 Ganeshpurkar A, Singh R, Singh RB, Kumar D, Kumar A& Kumar SS, Identification of potential AChE inhibitors through combined machine-learning and structure-based design approaches. *Indian J Biochem Biophys*, 59 (2022) 619.

7 Saffari-Chaleshtori J, Shafiee SM & Heidarian E, The effect of bilirubin on Bad, Bak, and Bim pro-apoptotic factors: A molecular dynamic simulation study. *Indian J Biochem Biophys*, 58 (2021) 236.

8 Srivastava S & Pandey A, Computational screening of anticancer drugs targeting miRNA155 synthesis in breast cancer. *Indian J Biochem Biophys*, 57 (2020) 389.

9 Katiyar K, Srivastava RK, Nath R & Singh G, Cryptosporidiosis, a public health challenge: A combined 3D shape-based virtual screening, docking study, and molecular dynamics simulation approach to identify inhibitors with novel scaffolds for the treatment of cryptosporidiosis. *Indian J Biochem Biophys*, 59 (2022) 296.

10 Erdogan T, Computational evaluation of 2-arylbenzofurans for their potential use against SARS-CoV-2: A DFT, molecular docking, molecular dynamics simulation study. *Indian J Biochem Biophys*, 59 (2022) 59.

11 Murugan NA, Chitra JP, Jeyaraman J & Rajendren SM, Multi-level scoring approach to discover multi-targeting potency of medicinal plant phytochemicals against protein targets in SARS-CoV-2 and human ACE-2 receptor. *Indian J Biochem Biophys*, 60 (2023) 1088.

12 Elgiushy H, Hammad S, Hassan A. S & Aboutaleb N, Acrylamide moiety, a valuable fragment in medicinal chemistry: insight into synthetic methodologies, chemical reactivity and spectrum of biological activities of acrylamide derivatives. *J Adv Pharm Res*, 2 (2018) 221.

13 Fu J, Cheng K, Zhang Z ming, Fang R qin & Zhu H liang, Synthesis, structure and structure–activity relationship analysis of caffeic acid amides as potential antimicrobials. *Eur J Med Chem*, 45 (2010) 2638.

14 Hu X, Tang S, Yang F, Zheng P, Xu S, Pan Q & Zhu W, Design, synthesis, and antitumor activity of olmutinib derivatives containing acrylamide moiety. *Molecules,* 26 (2021) 3041.

15 Gu X, Jiang Y, Chen J, Zhang Y, Guan M, Li X, Zhou Q, Lu Q, Qiu J & Yin X, Synthesis and biological evaluation of bifendate derivatives bearing acrylamide moiety as novel antioxidant agents. *Eur J Med Chem*, 162 (2019) 59.

16 Tanış E, Çankaya N & Yalçın S, Synthesis, characterization, computation of global reactivity descriptors and antiproliferative activity of n-(4-nitrophenyl)acrylamide. *Russ J Phys Chem,* B13 (2019) 49.

17 Elgiushy HR, Hammad SF, Hassan AS, Aboutaleb N & Abouzid K, Acrylamide moiety, a valuable fragment in medicinal chemistry: insight into synthetic methodologies, chemical reactivity and spectrum of biological activities of acrylamide derivatives. *J Adv Pharm Res*, 2 (2018) 221.

18 Vogel AI, Tatchell AR, Furniss BS, Hannaford AJ & Smith PWG, *Vogel's Textbook of Practical Organic Chemistry*, 5th Edition (1996).

19 Mazik M, Bläser D & Boese R, Hydrogen-bonding motifs in the crystals of secondary diamides with 2-amino-6-methyl- and 2,6-diaminopyridine subunits. *Tetrahedron*, 55 (1999) 12771.

20 Cakmak S, Kutuk H, Odabasoglu M, Yakan H & Buyukgungor O, Spectroscopic properties and preparation of some 2,3-dimethoxybenzamide derivatives. *Lett Org Chem*, 13 (2016) 181.

21 Frisch MJ, Trucks GW, Schlegel HB, Scuseria GE, Robb MA, Cheeseman JR, Scalmani G, Barone V, Mennucci B, Petersson GA, Nakatsuji H, Caricato M, Li X, Hratchian HP, Izmaylov AF, Bloino J, Zheng G, Sonnenberg JL, Hada M, Ehara M, Toyota K, Fukuda R, Hasegawa J, Ishida M, Nakajima T, Honda Y, Kitao O, Nakai H, Vreven T, Montgomery J. A. J, Peralta JE, Ogliaro F, Bearpark M, Heyd JJ, Brothers E, Kudin KN, Staroverov VN, Keith T, Kobayashi R, Normand J, Raghavachari K, Rendell A, Burant JC, Iyengar SS, Tomasi J, Cossi M, Rega N, Millam JM, Klene M, Knox JE, Cross JB, Bakken V, Adamo C, Jaramillo J, Gomperts R, Stratmann RE, Yazyev O, Austin AJ, Cammi R, Pomelli C, Ochterski JW, Martin RL, Morokuma K, Zakrzewski VG, Voth GA, Salvador P, Dannenberg JJ, Dapprich S, Daniels AD, Farkas O, Foresman JB, Ortiz J V, Cioslowski J & Fox DJ, Gaussian 09 (2013).

22 Dennington R, Keith T & Millam J, GaussView, Version 5 (2009).

23 Chang CE & Gilson MK, Tork: Conformational analysis method for molecules and complexes. *J Comput Chem*, 24 (2003) 1987.

24 BIOVIA DS, Discovery Studio Visualizer, v20.1.0.19295 (2016).

25 Blois MS, Antioxidant Determinations by the Use of a Stable Free Radical. *Nature*, 181 (1958) 1199.

26 Dechayont B, Ruamdee P, Poonnaimuang S, Mokmued K & Chunthorng-Orn J, Antioxidant and antimicrobial activities of pogostemoncablin (blanco)benth. *J Bot*, 2017 (2017) 1.

27 Re R, Pellegrini N, Proteggente A, Pannala A, Yang M & Rice-Evans C, Antioxidant activity applying an improved ABTS radical cation decolorization assay. *Free RadicBiol Med*, 26 (1999) 1231.

28 Andrews JM, Determination of minimum inhibitory concentrations. *J AntimicrobChemother*, 48 (2001) 5.

29 Morris GM, Huey R, Lindstrom W, Sanner MF, Belew RK, Goodsell DS & Olson AJ, AutoDock4 and AutoDockTools4: Automated docking with selective receptor flexibility. *J Comput Chem*, 30 (2009) 2785.

30 Trott O & Olson AJ, AutoDock Vina: Improving the speed and accuracy of docking with a new scoring function, efficient optimization, and multithreading. *J Comput Chem*, 31 (2010) 455.

31 Berman HM, Westbrook J, Feng Z, Gilliland G, Bhat TN, Weissig H, Shindyalov IN & Bourne PE, The Protein Data Bank. *Nucleic Acids Res*, 28 (2000) 235.

32 Kryger G, Silman I & Sussman JL, Structure of acetylcholinesterase complexed with E2020 (Aricept®): implications for the design of new anti-Alzheimer drugs. *Structure*, 7 (1999) 297.

33 Lindahl E, Abraham MJ, Hess B & D van der S, GROMACS 2020 Source code (2020).
34 Ponder JW & Case DA, Force fields for protein simulations. *Adv Protein Chem*, 66 (2003) 27.
35 Sousa Da Silva AW & Vranken WF, ACPYPE - AnteChamberPYthon Parser interfacE. *BMC Res Notes*, 5 (2012) 367.
36 Baker NA, Sept D, Joseph S, Holst MJ & McCammon JA, Electrostatics of nanosystems: Application to microtubules and the ribosome. *Proc Natl Acad Sci U S A*, 98 (2001) 10037.
37 Kumari R, Kumar R & Lynn A, G-mmpbsa -A GROMACS tool for high-throughput MM-PBSA calculations. *J Chem Inf Model*, 54 (2014) 1951.
38 Patil AS, Sayyed MM, Bhairamadgi NS, Han SH & Maldar NN, Synthesis and characterization of soluble polyamides from bis-[(4′-aminobenzyl)-4-benzamide] ether and various diacids. *Polym Bull*, 66 (2011) 1207.
39 CakmakS&Veysioglu A, Preparation, characterization and evaluation of some new amides as antimicrobial agents. *Hittite J Sci Eng*, 7 (2020) 345.
40 Kırca BK, Çakmak Ş, Kütük H, Odabaşoğlu M & Büyükgüngör O, Synthesis and characterization of 3-acetoxy-2-methyl-N-(phenyl)benzamide and 3-acetoxy-2-methyl-N-(4- methylphenyl)benzamide. *J Mol Struct*, 1151 (2018) 191.
41 Çakmak Ş, Novel diamide derivatives: synthesis, characterization, urease inhibition, antioxidant, antibacterial, and molecular docking studies. *J Mol Struct*, 1261 (2022) 132932.
42 Chakkaravarthi K, Krishnan KG, Gokulakrishnan K, Suman T & Tamilvendan D, Synthesize, spectral, antimicrobial andantioxidant studies of diamide mannich base derivatives. *Int J Pharm Pharm Sci*, (2014) 432.
43 Wu C, Pan Z, Yao G, Wang W, Fang L & Su W, Synthesis and structure–activity relationship studies of teixobactin analogues. *RSC Adv*, 7 (2017) 1923.
44 Santos MC, Botelho FD, Gonçalves AS, Kuca K, Nepovimova E, Cavalcante SFA, Lima ALS & França TCC, Theoretical assessment of the performances of commercial oximes on the reactivation of acetylcholinesterase inhibited by the nerve agent A-242 (novichok). *Food Chem Toxicol*, 165 (2022) 113084.
45 Chen Y, Fang L, Peng S, Liao H, Lehmann J & Zhang Y, Discovery of a novel acetylcholinesterase inhibitor by structure-based virtual screening techniques. *Bioorg Med Chem,* 9 (2012) 3181.